Contents lists available at ScienceDirect

Atmospheric Research

journal homepage: http://ees.elsevier.com

A multi-sensor and modeling analysis of a severe convective storm in Lake Maggiore area (northwestern Italy)

Elenio Avolio [a,*], Luca Nisi [b], Luca Panziera [b], Lionel Peyraud [c], Mario Marcello Miglietta [d]

[a] Institute of Atmospheric Sciences and Climate – National Research Council (ISAC-CNR), Lamezia Terme, Italy
[b] Federal Office of Climatology and Meteorology, MeteoSwiss, Locarno-Monti, Switzerland
[c] Federal Office of Climatology and Meteorology, MeteoSwiss, Geneva, Switzerland
[d] Institute of Atmospheric Sciences and Climate – National Research Council (ISAC-CNR), Padua, Italy

ARTICLE INFO

Keywords
Severe storm
Supercell
Mesocyclone
WRF
Deep convection
Lake Maggiore

ABSTRACT

The analysis of a severe convective storm, occurred in northwestern Italy during late summer 2012, is presented here. The event was characterized by heavy precipitation, hail and intense wind gusts, causing injuries and damages to trees, buildings and infrastructures.The description of the case study draws upon a wide palette of observational data. Surface and upper-air observations helped characterize the event, emphasizing the rapid changes in the meteorological parameters in the study area; satellite data highlights the presence of deep moist convection, associated with strong updrafts; Doppler radar allows the identification of the main features of the event in terms of storm-motion, hail detection/probability and the possible presence of a mesocyclone. A high-resolution (3 km inner grid spacing) simulation with the WRF (Weather Research and Forecasting) model was performed to study the atmospheric conditions conducive to convection, as well as to estimate the main instability parameters. The main features of the storm were well reproduced with WRF; furthermore, the high values of the simulated instability parameters denote the presence of favourable conditions for severe convection.The analysis of this event shows that supercells can develop also in a pre-alpine environment, characterized by a complex orography, in particular in the sub-regions where the local morphology creates conditions favourable for severe weather development.

1. Introduction

The Mediterranean basin is particularly prone to heavy rainfall and convective events, mainly due to the peculiar climatic characteristics of the region and to its complex morphology. Synoptic-scale patterns, Mediterranean cyclones or mesoscale convective systems (MCSs) may interact with local geographical and topographical features to develop severe weather, such as wind gusts, hail and tornadoes (Jirak et al., 2003; Schenkman et al., 2011; Jansà et al., 2014).

The inhomogeneous environment of the Mediterranean basin requires high-resolution analysis in order to take into account properly the interaction with the orography, the land–sea contrast, and the intense air–sea interaction (Lionello et al., 2006). These effects determine significant small-scale variations of the instability parameters, a peculiar feature compared to environments with a more homogeneous morphology, e.g. the U.S. Great Plains, where the typical horizontal scale of variation is generally much wider (Doswell III et al., 2012). Indeed, small-scale terrain features may be crucial in forcing local circulations, which, in combination with the presence of moist and warm air in the low levels, support the development of severe convection (Homar et al., 2003) and supercells (Scheffkneckt et al., 2017; Miglietta et al., 2016, 2017a, 2017b; Peyraud, 2013).

The Italian peninsula is occasionally affected by localized severe convective events associated with intense winds, such as tornadoes and downbursts. Historical documents and press news reveal that their occurrence is not rare, especially in specific sub-areas (e.g., Gianfreda et al., 2005). Such events are reported only rarely in official bulletins, since synoptic stations are too sparse to provide a detailed coverage of small-scale phenomena; thus, their occurrence is generally attested by amateurs' reports and dedicated forum websites. Several web portals/platforms that web surfers use to share and upload pictures and videos gather additional information even on weak events, which otherwise could not be reported. In the absence of photographs or videos to document their occurrence, as for night-time events, the damage survey is the best method to discriminate between a tornado and a straight-line wind event (e.g., a microburst).

* Corresponding author at: ISAC-CNR, c/o Area Industriale, compartment 15, I-88046 Lamezia Terme, Italy.
E-mail address: e.avolio@isac.cnr.it (E. Avolio)

https://doi.org/10.1016/j.atmosres.2020.105008
Received 9 January 2020; Received in revised form 21 April 2020; Accepted 24 April 2020
Available online xxx
0169-8095/

Using such unofficial data sources, a 10-year "climatology" of tornadoes and waterspouts in Italy was undertaken -some years ago (Giaiotti et al., 2007). The Po Valley, especially its eastern side, stood out as one of the Italian areas most affected by such events, primarily due to the contrast between the low-level relatively warm and moist air moving northward from the Adriatic Sea and the cold upper level air intrusions crossing the Alps. An updated climatology of tornadoes and waterspouts in Italy was recently provided (Miglietta and Matsangouras, 2018), including a classification of these events in terms of geographical, seasonal, monthly, diurnal, and rating distribution, for the period 2007–2016. The authors confirmed that these events are more frequent in late spring/summer in northern Italy, occurring mainly in flat areas or close to the coastlines. On average, the yearly density of tornadoes in Italy is comparable with that of other Mediterranean countries (Matsangouras et al., 2014, 2017; Rodríguez and Bech, 2018), but the frequency of occurrence may be much higher in specific sub-areas. Although statistics on downbursts in Italy are not available, the analysis of the ESWD (European Severe Weather Database; Dotzek et al., 2009) suggests that also "linear" storms (e. g., squall line) occur more frequently in summer in the Po Valley.

An intense event occurred in the pre-Alpine region during the evening of 25 August 2012, when a severe convective storm hit the Lake Maggiore area (northwestern Italy; Fig. 1), and in particular

Fig. 1. a) The two domains used in the numerical simulation. b) The innermost WRF grid and the model terrain height (m), including the location of the places mentioned in the manuscript. c) A zoom in the Lake Maggiore area, including the location of the places mentioned in the manuscript. d) A further zoom in the Verbania area; the zones affected by damages are coloured in red (the map was available on: http://www.verbaniamilleventi.org). e) and f) Damages near Villa Taranto. (For interpretation of the references to colour in this figure legend, the reader is referred to the web version of this article). (For interpretation of the references to colour in this figure legend, the reader is referred to the web version of this article.)

the town of Verbania (coordinates LON: 8.55°E, LAT: 45.92°N). The region of Lake Maggiore is not only one of the two regions with the largest amount of yearly precipitation in the Alps (Isotta et al., 2014), but is also particularly prone to precipitation episodes with high rainfall intensity (Panziera et al., 2018). Heavy rainfall events are usually triggered in the region by south-to-southeasterly mesoscale flows forced to ascend over the mountains in the northwestern side of the lake in a conditionally unstable environment (Panziera and Germann, 2010; Panziera et al., 2015). In the warm months, the area is also frequently affected by thunderstorms producing hail, in particular in the southeastern side of the lake (Nisi et al., 2016).

In the early afternoon, the thunderstorm of 25 August 2012 was triggered to the west-south-west of lake Maggiore, in the northern part of Novara province (Piedmont region; Fig. 1b), where only minor damages were reported; at around 18:00 UTC, the storm dramatically reinforced during its transit over the lake, remaining severe farther northeastward, in the northern part of the province of Varese and in southern Ticino, Switzerland, before weakening later in the evening. Torrential rain, with peaks of above 100 mm in 3 h (mainly concentrated in a band about 5 km wide), localized hail and strong gusts were reported in these areas. Several trees were uprooted, creating traffic problems and obstructing some minor rivers; public lighting was damaged; widespread damages to houses and cars were reported and power outages occurred. About twenty people were wounded, although not seriously.

As a consequence of the severe wind, the world-recognized botanic garden of Villa Taranto was destroyed, being 350 secular trees uprooted, for an estimated damage of more than 11 million euros. (Fig. 1e,f show some photos of the damages near Villa Taranto.) The area has not been immune to similar events in the past, since a severe wind gust (possibly a tornado) on 28 June 2006 uprooted some big trees in "Isola Madre" in the Borromeo Gulf (https://www.varesenews.it/2006/06/lago-maggiore-tromba-d-aria-sull-isola-madre/251863/).

The storm in Verbania was of smaller intensity compared to other severe localized storms that affected Italy in the last few years (Miglietta and Rotunno, 2016; Zanini et al., 2017), but its peculiarity was that it occurred in the area of Lake Maggiore, a prealpine area where rotating storms have not yet been documented in the literature so far, even though convective storms are frequent (Nisi et al., 2016). We consider this event worth of investigation also due its good radar data coverage, in particular the Monte Lema MeteoSwiss radar located on the northern side of Lake Maggiore and the radar of the Piedmont region in Bric della Croce (which, with the radar of Monte Settepani, constitutes the radar Piedmont mosaic), although the latter is too far south to provide very detailed information.

Therefore, the purpose of the present paper is twofold: on the one hand, we will identify the characteristics of this storm, also using recently developed detection algorithms, in order to better understand the characteristics of the environment where the supercell developed; on the other hand, we will explore how far we can go in the prediction of this kind of events using limited area models. This is particularly relevant in the Alpine area, where supercells have been documented in the literature only in a few cases; therefore, we believe that our analysis, even if limited to a single case study, can provide valuable information for the study and the prediction of similar events in the region.

The summary of the present paper is the following: after a synoptic analysis of the event in Section 2, some surface observations and a nearby sounding are analysed in Section 3. Then, a satellite perspective of the case study is provided in Section 4 and radar data are discussed in Section 5, in order to identify the main features of the event using different data sources. In Section 6, limited area model simulations are examined, focusing on some instability parameters in order to estimate the potential instability of the surrounding environment. Conclusions are drawn in Section 7.

2. Synoptic conditions

Considering the fields at 00:00 UTC, 26 August 2012, a levelled field of the mean sea level pressure was apparent over northern Italy (Fig. 2). This configuration followed several days characterized by a persistent African anticyclone affecting the western Mediterranean region; such conditions favoured the accumulation of moist and warm air at low levels. Meanwhile, a frontal system affected the Alpine region, slowly moving southeastward. The front separated the colder air north of the Alps (bluish colours in Fig. 3) from the warmer Mediterranean air on its southern side (reddish colours).

The cooler air mass slowly penetrated from the Alpine region toward the Po valley (Fig. 1b), producing a temperature decrease of a few K over northwestern Italy: e.g., at 850 hPa, a decrease of 4 K was observed in 12 h (Fig. 3), and a similar change was observed at upper levels (not shown). The combination of upper level cold air and pre-existing very hot and moist low-level air increased the potential instability of the environment. Also, the right-entrance of an upper level southwesterly jet streak (Fig. 4), located near the Lake Maggiore area, favoured large-scale ascending motion.

Looking at the geographic distribution and timing of lightning activity recorded by the LINET network (Betz et al., 2009), one may identify a strong convective signal elongated in southwest/northeast direction from the central part of Piedmont region toward the Lake Maggiore area, where the lightning activity reached its maximum, and farther northeastward (Fig. 5).

3. Surface observations and radiosounding

The intensive wind-induced damages confined in a limited area suggest that the event was characterized by high wind speeds associated to a localized convective event; however, it remained unclear whether it was a tornado or a downburst. The inspection of most trees uprooted during the event and the prevailing direction along which they were inclined, from southwest to northeast, i.e. along the large-scale wind direction, suggest that the system was linear. Also, some employees of the Lake Maggiore navigation company confirmed the presence of a frontal line propagating along the lake, accompanied by rain and wind gusts (personal communication). However, a damage survey performed by one author of the present paper revealed that in some areas of Pallanza the damages were more scattered (see also Fig. 1d) and the trees were inclined in different directions, thus suggesting the possible presence of a tornado, probably coexisting with the downburst. Further discussion on this point will be provided with the support of radar data in Section 6.

The data from the surface station meso-network of the Piedmont region and the meteorological radar system, consisting of two polarimetric radars and a mobile X-band radar, which is part of the national surveillance network, are considered for precipitation analysis. Very intense rainfall concentrated for a few hours in a very narrow band, extending over the Alpine foothills from Biella to Lake Maggiore and Ticino areas (Fig. 1); the highest rainfall amount occurred in the provinces of Verbania and Biella with a maximum of about 93 mm in 3 h and widespread hail (up to 6 cm, as discussed in Section 7) in these two areas (ARPA Piemonte, 2012). According to a detailed analysis of the storm cells detected by the radar system (see Section 5), the hail formed at a high altitude, due to the elevated height of the 0 °C isotherm, and reached the ground partially fused and mixed with rain.

The anemometer in Verbania Pallanza, located at the headquarters of ISE-CNR (Institute for the Study of Ecosystems – National Research Council), in front of the Borromeo Gulf (Fig. 1c), recorded a

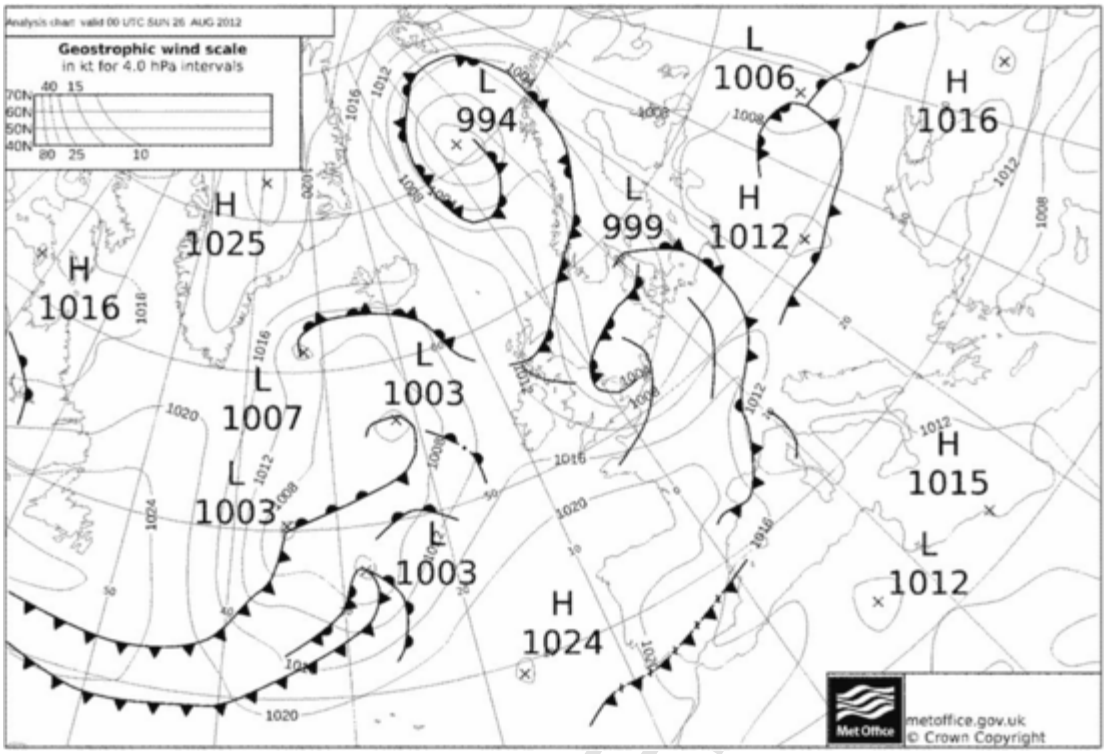

Fig. 2. Surface map (sea level pressure [hPa] and weather fronts) at 00:00 UTC, 26-08-2012 (source: metoffice.gov.uk).

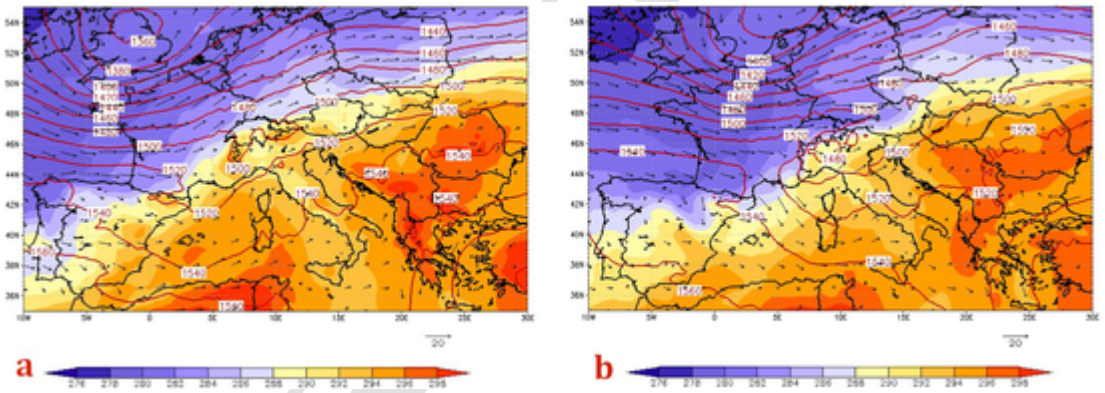

Fig. 3. 850 hPa Temperature (colours, °C), geopotential height (red-contours, m) and wind vectors (m/s): 12:00 UTC, 25-08-2012 (left) and 00:00 UTC, 26-08-2012 (right). The maps are derived from Global Forecast System (GFS) analysis at 0.5° horizontal resolution. (For interpretation of the references to colour in this figure legend, the reader is referred to the web version of this article). (For interpretation of the references to colour in this figure legend, the reader is referred to the web version of this article.)

wind gust during the event, of about 30 m/s (about 108 km/h), at 17:58 UTC (Fig. 6). The damages in the immediate surroundings of the station were relatively minor and consistent with this measure (e.g., the storm caused the breakup of some windows in the institute and the removal of few roof tails in some houses in the surroundings). However, the damage survey suggested that the most intense part of the thunderstorm struck 1 km farther away, in the gardens of Villa Taranto (Fig. 1c), where hundreds of large trees were snapped and uprooted (damage indicator 27, degree of damage 3 and 4; McDonald and Mehta, 2006), suggesting that a realistic estimation of the maximum wind gust should be of about 170–220 km/h (between the upper Enhanced Fujita scale EF1 rating and EF2).

Fig. 6 shows that, in correspondence with the peak in wind speed, a discontinuity was present in the wind direction, as the winds rotated from northeasterly to southwesterly and, then, back to northeasterly. The 2 h-cumulated precipitation from 17:30 UTC to 19:30 UTC was about 77 mm, but a notable peak of 11.2 mm was measured in 2 min immediately after the wind gust (Fig. 7). The descent of the cooler upper level air in the downdraft and the evaporation of precipitation were responsible for a 2 m temperature drop of about 12 °C in 3.5 h (5.5 °C from 17:30 to 18:30 UTC).

A pre-convective proximity thermodynamic sounding in Cuneo-Levaldigi at 10:00 UTC, 25 August 2012 is shown in Fig. 8 (source: Department of Atmospheric Science, University of Wyoming). The sounding is located upwind of the event, thus it may represent the characteristics of the environment before the occurrence of the storm (the sounding of Milano-Linate is located downstream of the storm, thus it is not representative of the environment preceding the event). The profile contains a very warm and moist boundary layer up to about 850 hPa, above which a thermal inversion delimits a shallow layer of warm and dry air; in the mid-levels, steep lapse rates are present in a deep layer. Such profiles are prototypical of the so-called "loaded gun" sounding configuration (Wallace and Hobbs, 2006), a characteristic of an unstable but capped air mass. In the

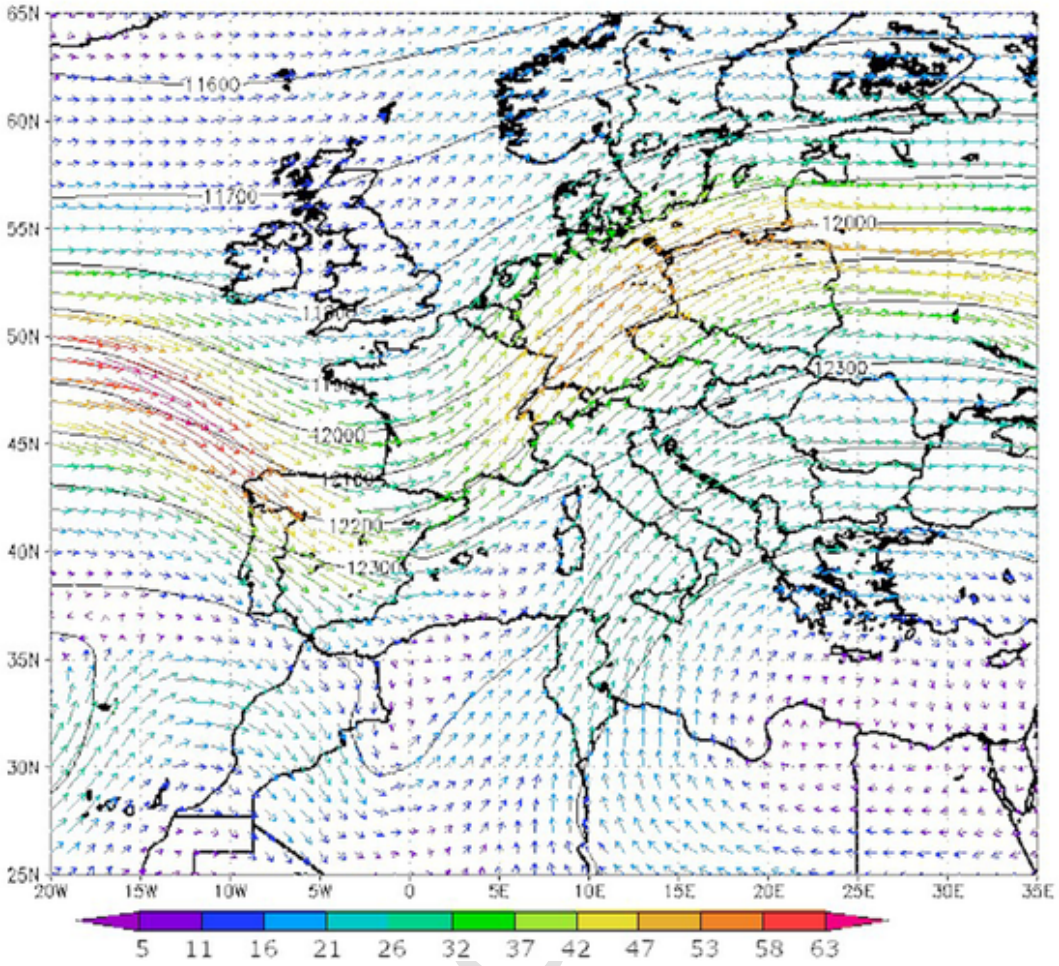

Fig. 4. 200 hPa geopotential height (black lines, m) and wind (coloured vectors, m/s) at 18:00 UTC, 25-08-2012. The map is derived from the GFS analysis at 0.5° horizontal resolution. (For interpretation of the references to colour in this figure legend, the reader is referred to the web version of this article).

sounding of Fig. 8, the surface-based CAPE (Convective Available Potential Energy) of the most unstable parcel is high (1984 J/kg) and a mechanical forcing of a few hundred meters should be able to overcome the convective inhibition and to release the layer instability.

We speculate that this was indeed the case: Lake Maggiore near Verbania is located just downstream of Mottarone mountain (1500 m high) with respect to the synoptic southwesterly flow. While the orography triggered convection, the evaporation from the lake locally enhanced the low-level humidity compared to that of the sounding in Fig. 8, which is representative of inland, drier conditions. This effect is emphasized in the Borromeo Gulf, where the orography surrounds three quarters of the water body and favours the persistence of warmer and more humid air (in Verbania Pallanza, the observed relative humidity at 17:30 UTC was 87%). As a consequence, near the lake the low-level dewpoint temperature profile would shift to the right compared to Fig. 8, hence increasing CAPE and reducing convection inhibition (CIN). The presence of more favourable low-level environmental conditions near the lake and the arrival of cooler air at 850 hPa contributed to the removal of the inversion in the Verbania area, thus allowing an explosive triggering of convection. Furthermore, the presence of intense vertical wind shear, both in the lowest 3 km and in the 0–6 km layer (from the sounding derived by the Department of Atmospheric Science, University of Wyoming, it follows that the 0–3 km (0–6 km) wind shear is about 17 m/s (33 m/s)), favoured the development of a supercell.

4. Satellite perspective

The sequence of colour-enhanced IR10.8 band satellite images from Meteosat-8 Rapid Scan Mode (Fig. 9) shows that the storm responsible for the damages in Verbania had very cold (215 K) cloud top temperatures (CTTs). An explosive convective process caused a rapid decrease of CTT between 17:35 UTC and 18:15 UTC. In particular, between 17:50 and 18:10 UTC, an extended portion of the cloud top showed a remarkable temperature decrease from 215 K to 202 K. After this rapid cooling, the storm showed a cold-U shaped signature (18:20 UTC), which then developed into a cold-ring shaped signature (18:25–18:30 UTC). These patterns indicate that severe convective processes are taking place (Brunner et al., 2007). The very low values of CTT are indicative of a very intense updraft, which determined a significant penetration of the upper part of the storm top into the warmer lower stratosphere (Setvák et al., 2010). Although not visible in the image, the data show that the coldest temperatures of the U- and V-shaped signatures are located slightly upwind (in this case on the southwestern side) of the overshooting top (OT), while the related cold protuberances extend downwind of the OT, along the perimeter of the cirrus anvil. Usually, storms showing these signatures are present within some specific air mass types, with a relatively weak upper-level wind shear and a strong thermal inversion above the tropopause (Setvák et al., 2010). These signatures are usually short-lived, because they are dependent on the duration of the OT of the cloud: the warm spot, which is lo-

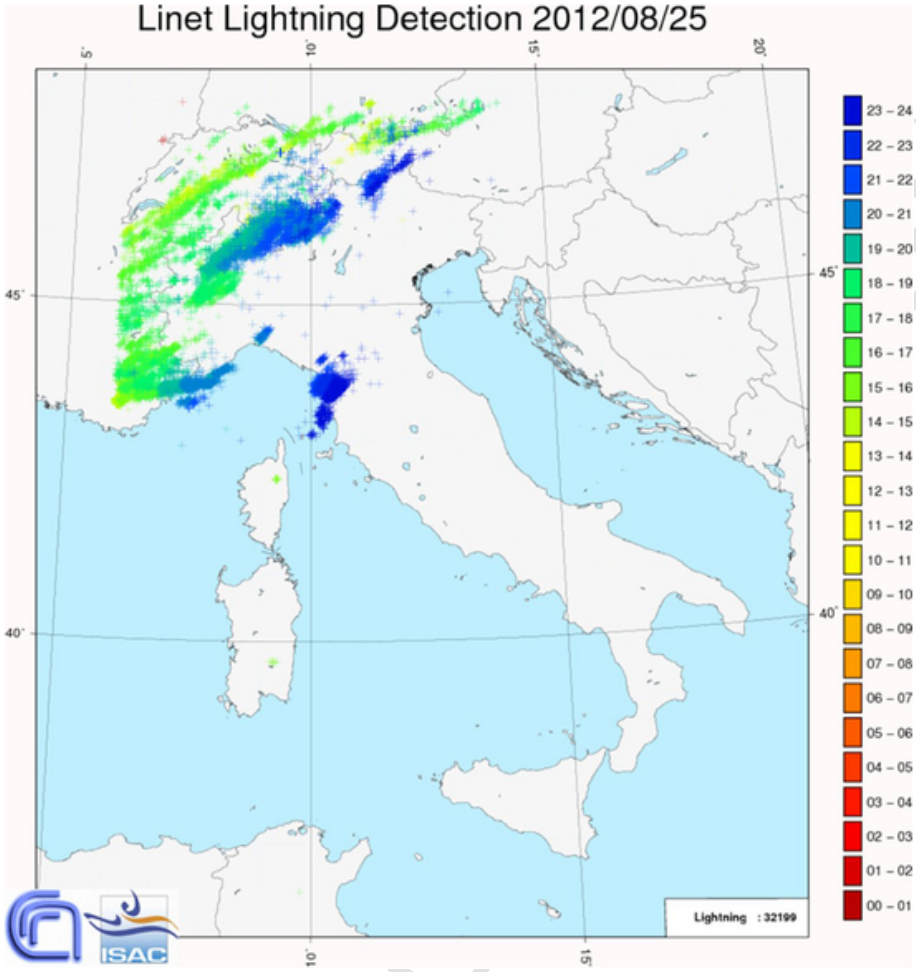

Fig. 5. Lightning activity (cloud-to-ground and intra-cloud) on 25-08-2012. The colours are representative of the different hours (UTC) of the day (courtesy of Satellite Meteorological Group of CNR-ISAC in Rome). (For interpretation of the references to colour in this figure legend, the reader is referred to the web version of this article).

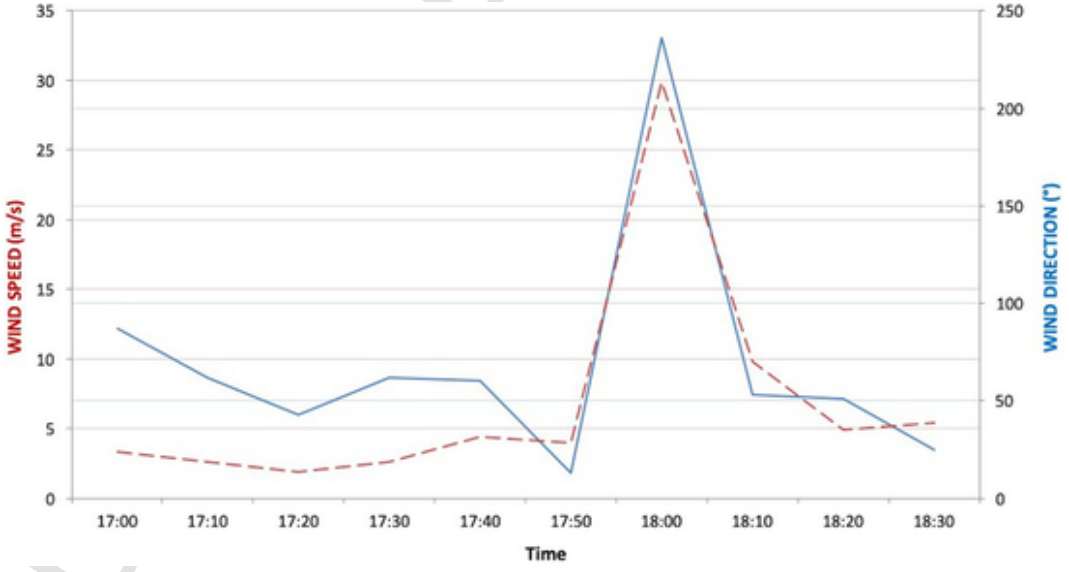

Fig. 6. 10 m wind speed (red dotted line, m/s) and direction (blue solid line, deg) recorded in Verbania from 17:00 UTC to 18:30 UTC. Data are instantaneous and reported every 10 min; the maximum wind registered at 17:58 UTC is included instead of the data at 18:00 (8.1 m/s). (For interpretation of the references to colour in this figure legend, the reader is referred to the web version of this article.)

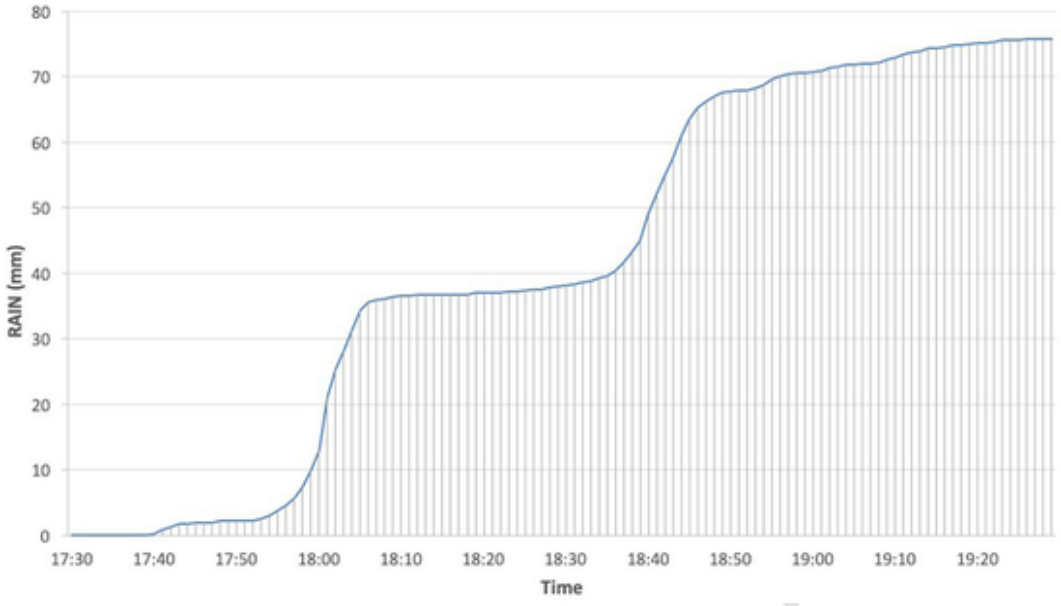

Fig. 7. Cumulated rainfall (mm) recorded in Verbania from 17:30 UTC to 19:30 UTC. Data are registered every minute.

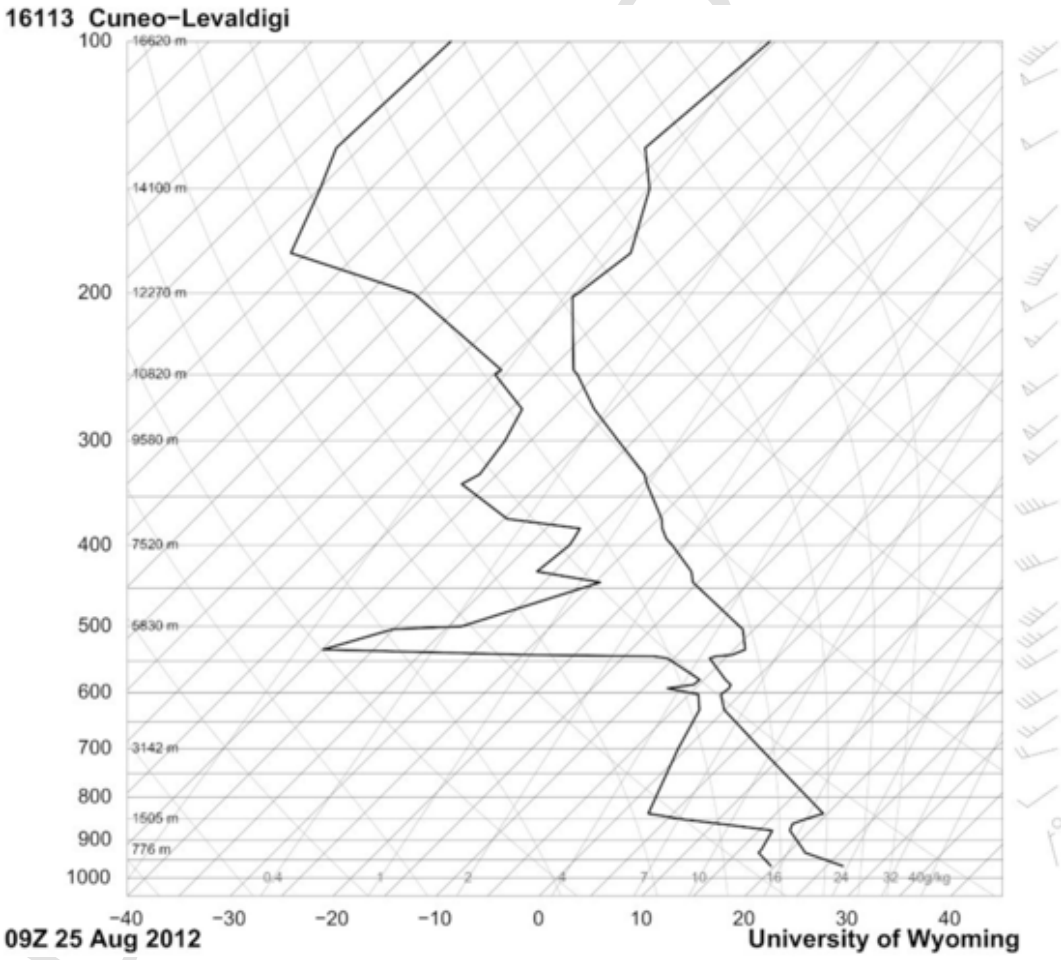

Fig. 8. Skew-T diagram in Cuneo-Levaldigi on 25 August 2012, 10:00 UTC (Source: Department of Atmospheric Science, University of Wyoming).

cated downwind, disappears when the OT decays. By analysing the images sequence, cold U-shaped or cold-rings signatures persisted between 17:35 and 18:30 UTC, confirming that the environment was very favourable to the development of severe convection.

5. Doppler analysis, radar tracking and hail

The radar analysis of the storm is performed using reflectivity and Doppler velocity images of the C-band radar operated by Me-

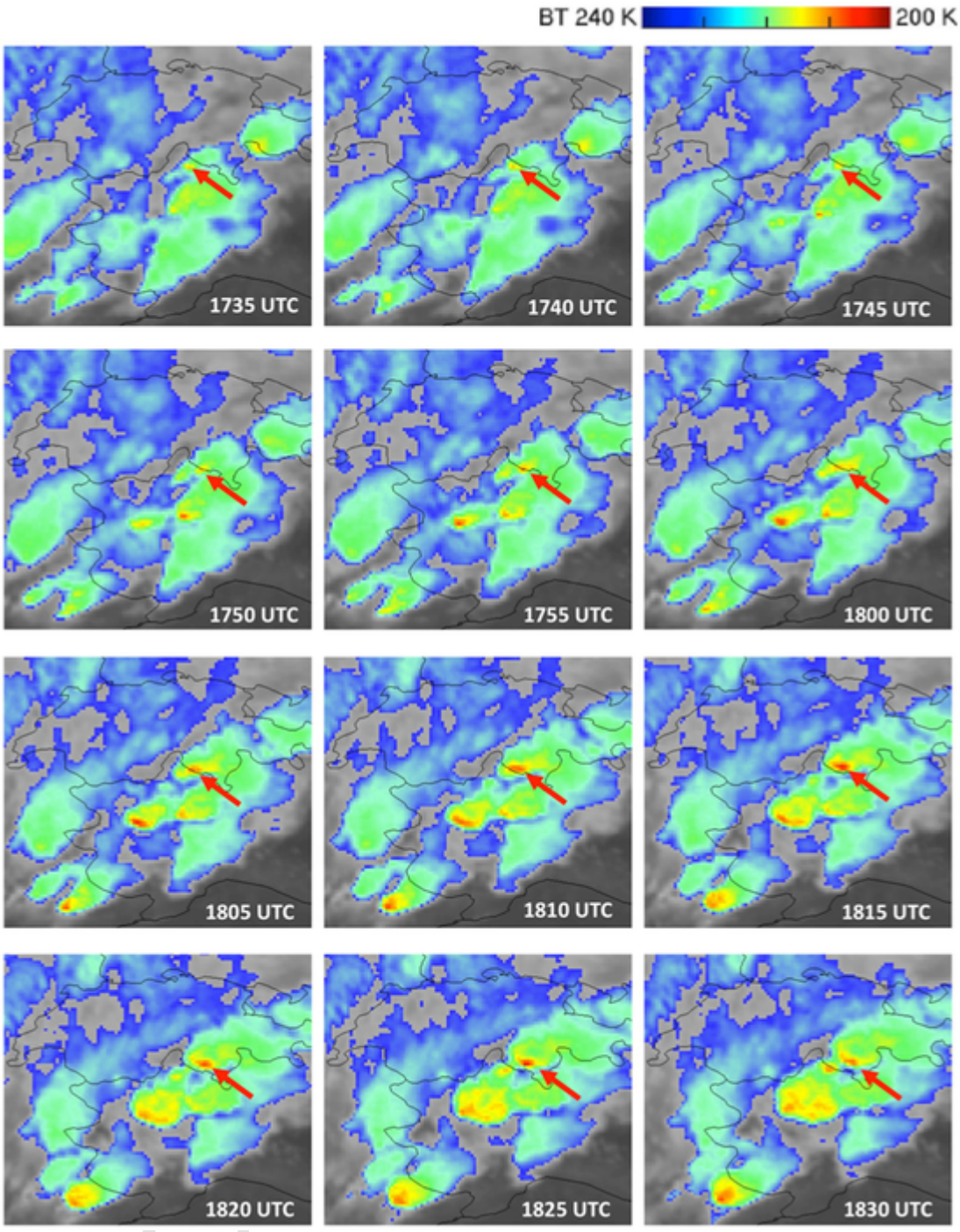

Fig. 9. Storm evolution over the Alpine region on 25 August 2012, 17:35–18:30 UTC. The Meteosat-8 colour-enhanced IR10.8 band shows a synchronized development of three severe storms. The uppermost storm, highlighted with the red arrow, is analysed in this manuscript (images are not parallax-corrected). (For interpretation of the references to colour in this figure legend, the reader is referred to the web version of this article). (For interpretation of the references to colour in this figure legend, the reader is referred to the web version of this article.)

teoSwiss, located just 30 km northeast of the city of Verbania on the top of Monte Lema (Fig. 1c), at 1600 m asl. The Swiss radar network is composed of five polarimetric C-band Doppler radars (Germann et al., 2015). The operational scan strategy of the Swiss radars consists of 20 elevation between −0.2° and 40° repeated every 5 min.

Fig. 10 shows the time sequence of reflectivity and Doppler velocity measured by the Monte Lema radar from 17:50 to 18:10 UTC, when the thunderstorm approached the Lake Maggiore and crossed the Borromeo Gulf near Verbania. Between the radar site and the location of the thunderstorm there are no mountains that may corrupt the data. Since the elevation of the radar beam is 2.5°, these images represent the storm at altitudes between 3 km asl (at 17:50 UTC) and 2.5 km asl (at 18:10 UTC). Even though there are some missing gates in the radar data, the reflectivity fields show the development of an intense thunderstorm with a hook-echo feature at 18:05 UTC. The reflectivity values are not extreme; however, they are larger

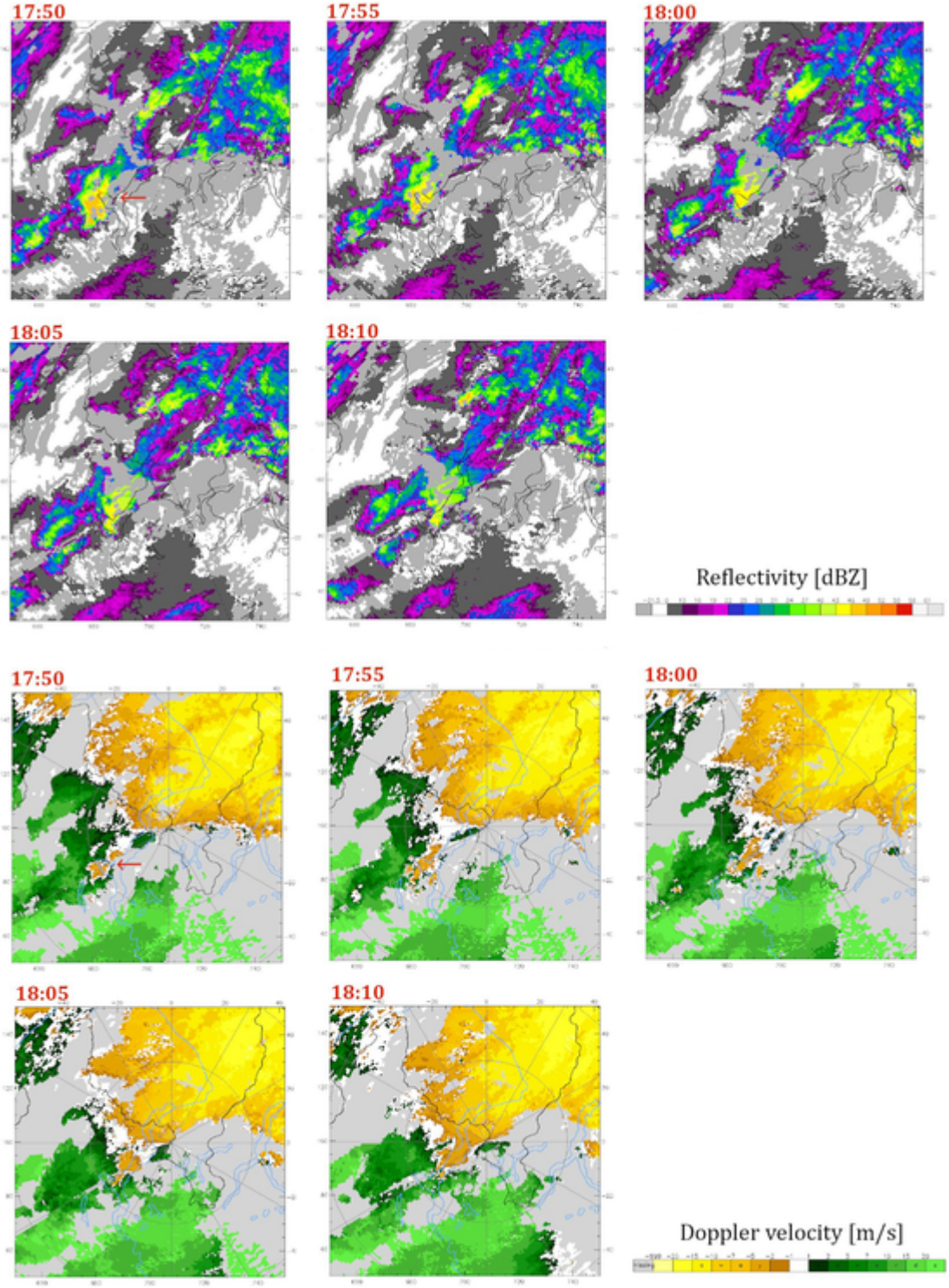

Fig. 10. Time sequence (17:50–18:10 UTC, 25 August 2012) of reflectivity (top, dBZ) and radial Doppler velocity (bottom, m/s), measured by the Monte Lema weather radar, at 2.5° elevation angle. The red arrows in the two 17:50 - panels indicate Verbania. The rings indicate the distances of 30 km and 60 km from the radar site. Positive values of Doppler velocity denote a wind that moves toward the radar, while negative values indicate a wind moving away from the radar. (For interpretation of the references to colour in this figure legend, the reader is referred to the web version of this article). (For interpretation of the references to colour in this figure legend, the reader is referred to the web version of this article.)

than 43 dBZ, with peak values of about 50–55 dBZ at an elevation higher than 2.5°.

The radial Doppler velocity field clearly shows an area of outbound flow within the larger mesoscale inbound wind, which indicates the presence of rotation associated with a mesocyclone. The gradual transition between the greenish and yellow colours in the area of rotation demonstrates that the algorithm used for the dealiasing of the radial wind field (James and Houze, 2001) produced a realistic field even in the presence of the strong directional gradients associated with the thunderstorm. The area of rotation is apparent in

multiple volume scans and extends from about 1.5 km - the lowest height visible with the radar - to about 4 km (not shown), thus enhancing the confidence that this feature is representative of a mesocyclone.

Although the radar in Bric della Croce (Piedmont region) was too far southwest with respect to Verbania for a detailed analysis of the storm, we show the Doppler velocity map at 18:00 UTC, 25 August 2012, to support our hypothesis of the presence of a mesocyclone. Fig. 11 shows an area of inbound flow near the region with the maximum reflectivity, suggesting a probable mesocyclonic rotation above the eastern side of Lake Maggiore.

The storm has also been analysed with the Thunderstorm Radar Tracking algorithm (TRT hereafter), a three-dimensional multiple-radar tracking used operationally at MeteoSwiss for thunderstorms nowcasting and storm climatological analysis (Hering et al., 2008). TRT is a two-step algorithm: the first part provides 2D storm-objects and related geographical and geometric information ("tracking"). The second part estimates the severity of the detected storms by including 3D radar data ("ranking"). The TRT output from the first step is used here to reprocess radar data and combine the track information with hail information provided by radar-based hail products (Nisi et al., 2018).

The storm initiated about 30 km southwest of Verbania at about 16:30 UTC (Fig. 12). Within moderate southwesterly steering winds, the storm reached the Verbania area in approximately one hour. Initially, the storm was rather weak and the probability of hail was low. By the time the storm approached the Lake Maggiore, the hail signal intensified considerably and reached POH (probability of hail) values greater than 70% over a large area as the storm moved northeastward. The intensification of storms near large lakes is a common occurrence in the southern Prealpine region (MeteoSwiss forecasters, personal communication): because of very moist low levels, the storm ingests a large amount of humid air in the updraft, which in turn can enhance the latent heat release, hence the updraft intensity.

The fact that the probability of hail was high over a large area near Verbania indicates that at that time the updraft of the storm was well organized and strong enough to sustain a hail core. Stronger and persistent updrafts allow the creation of hail cores and hail stone growth in the wet and dry accretion zones in storms. This process is especially efficient in the presence of large amounts of supercooled droplets, which are a consequence of intense updrafts ingesting large amounts of humidity and increasing the buoyancy because of the large latent heat release (due to condensation and glaciation processes). The more persistent the hail core is, the greater the possibility for hailstones to increase in size. The estimation of hail sizes, provided by the MESHS algorithm (Maximum Estimated Severe Hail Size, not shown here; Nisi et al., 2018) shows that over Verbania hail stones were rather small (< 2 cm). Larger hail sizes were apparent only at later stages, 20–30 min after the storm passed over Verbania. This most likely indicates that, at the time of the passage near Verbania, the hail core in the storm was rather young and the intensification of the updraft was probably quite recent and ongoing. The results of the algorithm are consistent with ESWD reports, which identify large hailstones only along the east coast of the Lake Maggiore and farther eastward.

6. Mesoscale model analysis

The fully compressible, non-hydrostatic WRF-ARW (Advanced Research WRF) model (Skamarock et al., 2008) version 3.9.1 is used here for the numerical simulation of this case study, in order to identify the atmospheric conditions responsible for severe convection and for the development of the supercell.

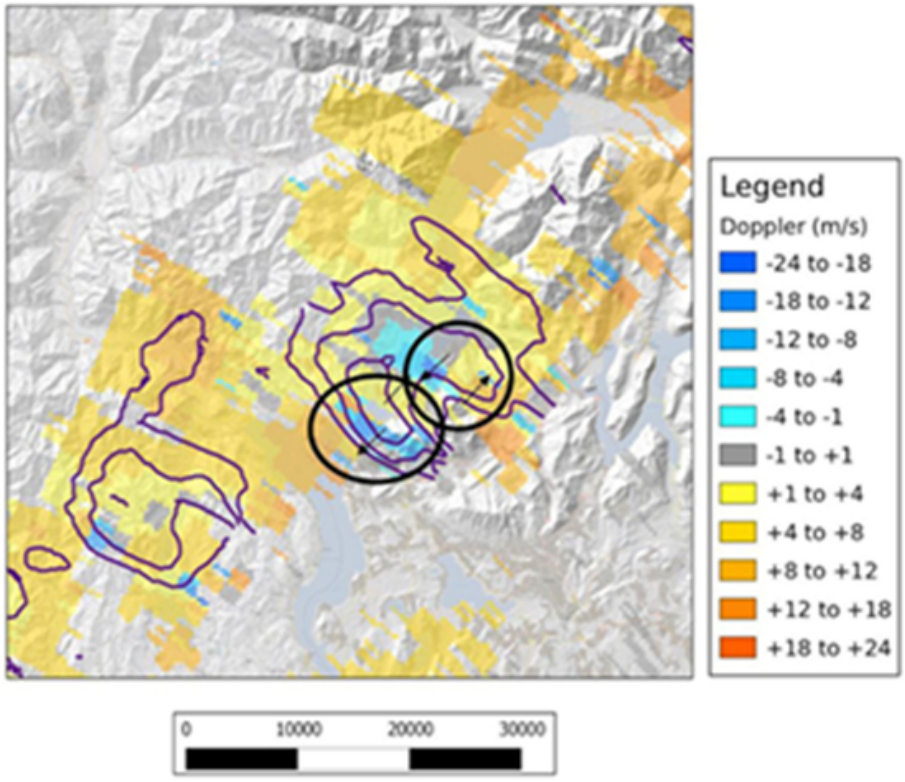

Fig. 11. Doppler velocity (m/s) measured by the "Bric della Croce" radar operated by ARPA Piedmont, on 25 August 2012, 18:00 UTC, at 0.5° elevation angle. The radar is located about 119 km southwest to Verbania (outside the domain shown in the Figure). Positive values of Doppler velocity denote a wind that moves away from the radar, while negative values indicate a wind toward the radar. The regions of probable mesocyclonic rotation are circled (black circles). The contour lines of reflectivity, with values higher than 56 dBZ, are also superposed on the map. (For interpretation of the references to colour in this figure legend, the reader is referred to the web version of this article).

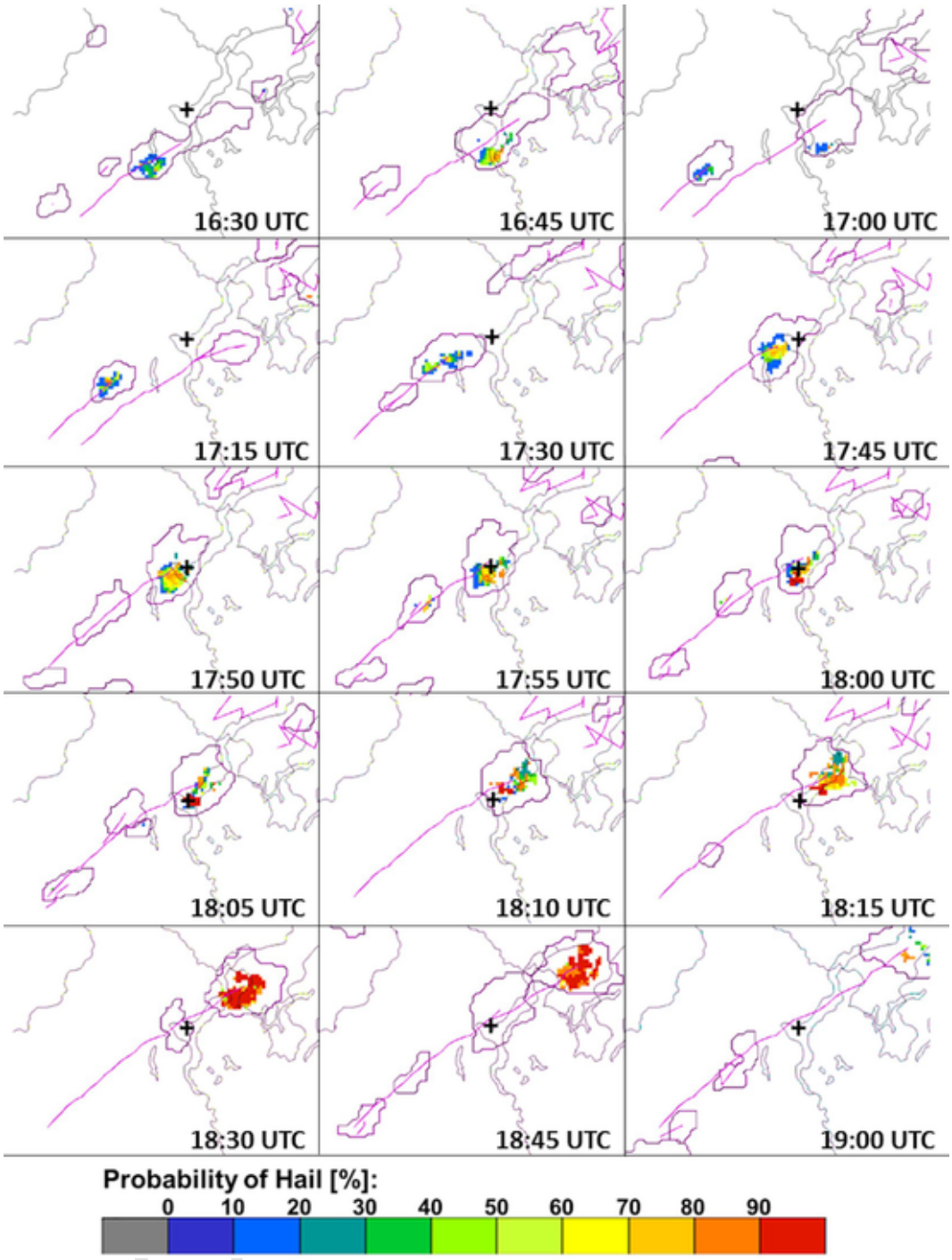

Fig. 12. Storm tracking (16:30–19:00 UTC) with the Thunderstorm Radar Tracking algorithm (Hering et al., 2008) and hail detection. The cell analysed in this study initiated in the area located west-southwest of Lake Maggiore. Colours inside the storms show the probability of hail (POH) (%). The Figure shows a rapid increase in the hail activity in the close proximity of Verbania (black 'plus sign' on the maps). (For interpretation of the references to colour in this figure legend, the reader is referred to the web version of this article).

6.1. Set-up

Two two-way nested domains are used for the simulation (Fig. 1a); the parent domain covers the central Mediterranean and the Italian peninsula (9 km grid spacing in both N-S and W-E directions; 192 × 184 grid points), while the second grid is centered over northwestern Italy (3 km grid spacing; 181 × 178 grid points). An additional WRF model simulation has been undertaken including a third domain, with grid spacing of 1 km, centered in the Lake Maggiore area and nested into the inner domain in Fig. 1a. However, results did not change significantly compared to those in the second grid (shown here), and are not discussed in the present study.

The model is implemented with 40 terrain-following vertical levels more closely spaced in the boundary layer, fifteen of them below 2000 m height. The simulation starts at 12:00 UTC, 24 August, and lasts 36 h; outputs are saved every half an hour. Initial and boundary conditions are derived from the National Center for Environmental

Prediction - Global Forecast System (NCEP-GFS), from the analysis cycle issued at 12:00 UTC, 24 August (0.5° horizontal resolution, fields every 3 h).

The model configuration follows that used in Avolio et al. (2017), about the sensitivity of boundary layer variables to different parameterization schemes, and in Avolio and Federico (2018), relative to the simulation of an extreme convective event in the Mediterranean. Thus, the physical parameterizations are: the new Rapid Radiative Transfer Model (RRTMG) long-wave and short-wave radiation scheme (Iacono et al., 2008), the Noah land-surface model (Tewari et al., 2004), the Thompson microphysics scheme (Thompson et al., 2008), the Asymmetrical Convective Model version 2 (ACM2) scheme (Pleim, 2007) for the PBL, and the Betts–Miller–Janjić (BMJ) cumulus parameterization (Betts and Miller, 1986). The latter is activated only for the coarse grid, while convection is explicitly resolved for the fine grid.

6.2. Precipitation patterns

Figs. 13 and 14 show respectively the maximum reflectivity (observed at 18:45 UTC in radar images and simulated at 18:30 UTC in the WRF run, inner grid) and the six-hour accumulated precipitation (simulated and observed) during the heavy rain event.

Fig. 13 shows a good qualitative agreement. In particular, the band of high reflectivity covering the northern parts of Piedmont, with a local maximum over Ticino, and that extending on the northern side of Liguria are well reproduced (although the simulated field is slightly more extended toward the northeast).

In Fig. 14a, the 6-h accumulated precipitation field, from 18:00 to 24:00 UTC on 25 August, is derived from the automatic system "Dewetra" (www.mydewetra.org), an integrated system of the Functional Center of the Italian Department of Civil Protection (DPC), through the interpolation of the rain gauge measurements of the national automatic stations. Apparently, the model underestimates the intensity of the rainfall (Fig. 14b; the 3 km grid field is shown) in its western side, while the agreement is better in the Lake Maggiore area, where a rain band oriented in the SW-NE direction and the areas of no rain on its south and NW side are well reproduced. In general, the whole simulated precipitation pattern, whose shape and maximum intensity are well reproduced, appears slightly shifted to northeast with respect to the observations.

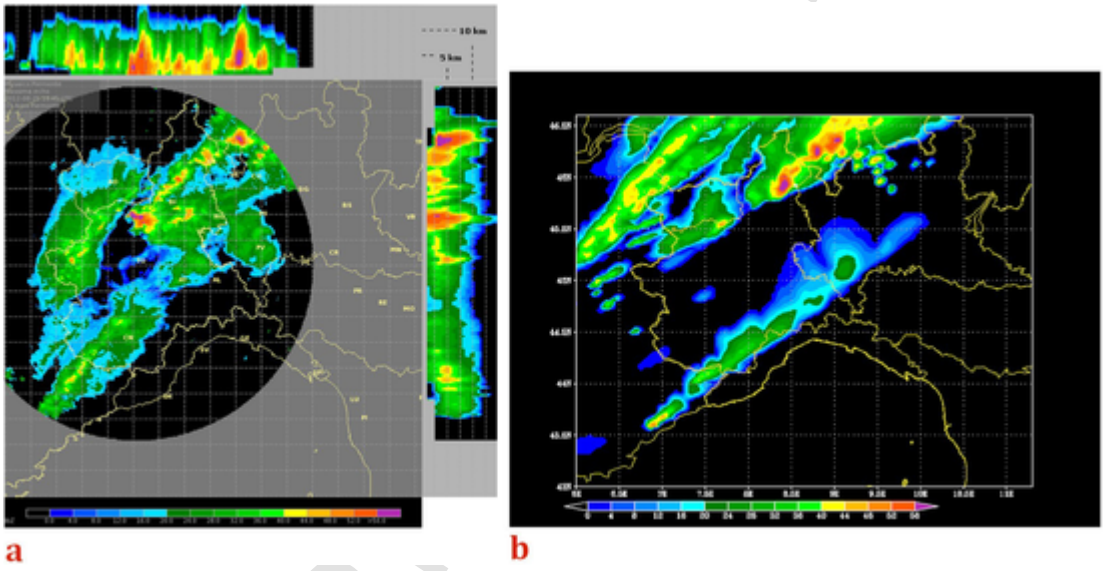

Fig. 13. Left: radar reflectivity (at 18:45 UTC, 25 August; data from the Piedmont mosaic, dBZ); right: 3 km grid maximum reflectivity (dBZ) simulated by the WRF model (at 18:30 UTC, 25 August). (For interpretation of the references to colour in this figure legend, the reader is referred to the web version of this article).

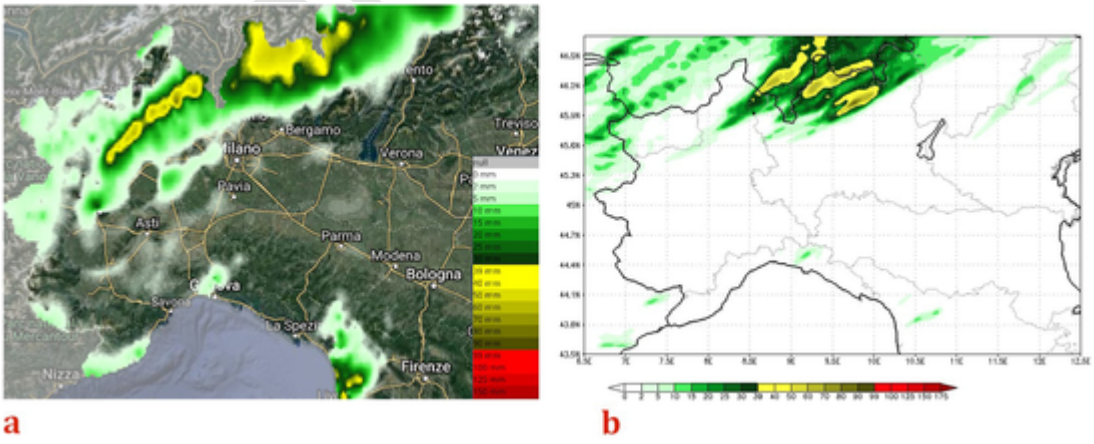

Fig. 14. Left: 6 h cumulated rain (mm/6 h) recorded by automatic stations (data from the automatic system "Dewetra" of the Italian Department of Civil Protection; www.mydewetra.org); right: 6 h cumulated rain (mm/6 h) simulated by the WRF model (3 km grid spacing). Both fields are shown at 00:00 UTC, 26 August. The black dot denotes the position of Verbania. (For interpretation of the references to colour in this figure legend, the reader is referred to the web version of this article).

Concerning available surface observations (Verbania Pallanza and Mottarone meteorological stations), although a punctual comparison is out of the scope of this work, we can see that the cumulated rain was generally underestimated by the model; e.g., in Verbania WRF simulated a daily precipitation of 31 mm (vs. 94 mm observed) and in Mottarone 28 mm (vs. 52 mm observed). Concerning the surface temperature, min/max values of 18.2/28.9 °C (17.6/29.7 °C) were simulated (observed) in Verbania. Finally, the observed wind gust, being associated with a local event (time evolution of a few minutes), was not reproduced by the model.

The vertical cross sections of equivalent potential temperature and of the vertical wind component are shown at Verbania latitude, 45.92°N in Fig. 15 (along the black line drawn in Fig. 16). The frontal system approaches from the west: the intrusion of cooler air

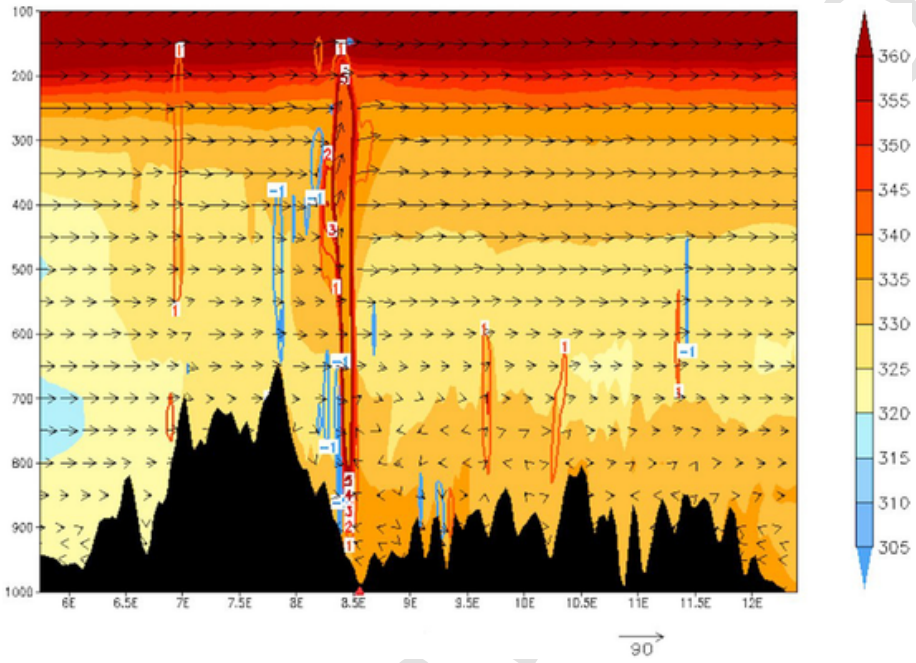

Fig. 15. WRF vertical cross section: equivalent potential temperature (shaded, K), vertical wind component (red contours for positive values, blue for negative; m/s), wind vector in the x-z plane at 18:30 UTC, 25 August. On the x-axis the longitude is reported (deg) and on the y-axis the pressure levels (mbar); the red triangle on the x-axis refers to the longitude of Verbania. (For interpretation of the references to colour in this figure legend, the reader is referred to the web version of this article). (For interpretation of the references to colour in this figure legend, the reader is referred to the web version of this article.)

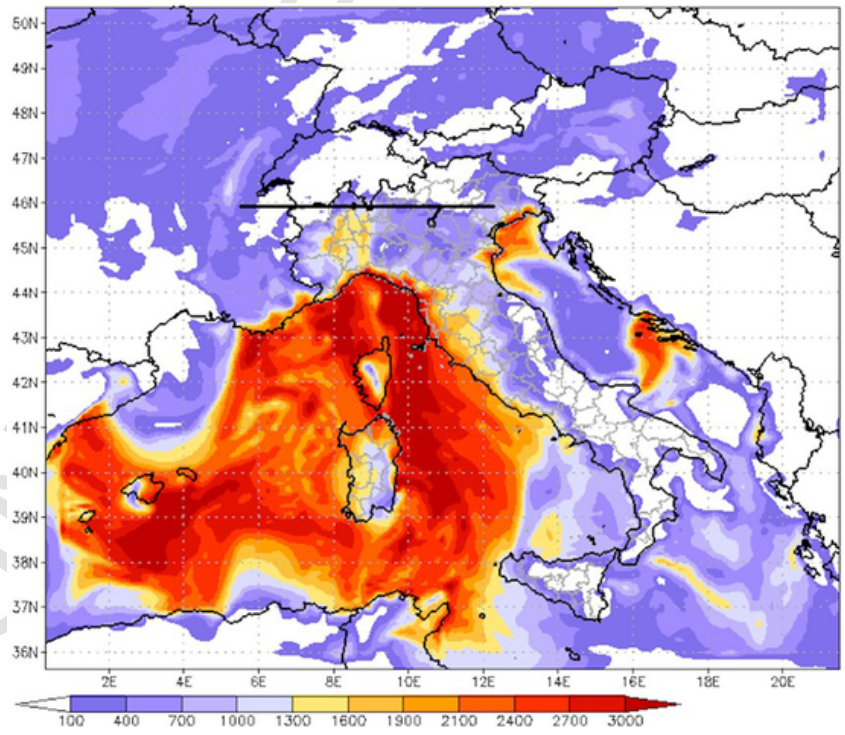

Fig. 16. WRF-outer grid most unstable CAPE (J/kg) at 18:00 UTC, 25 August. A black line is drawn to identify the cross section in Fig. 15. (For interpretation of the references to colour in this figure legend, the reader is referred to the web version of this article).

in mid-troposphere is visible on the left side of the Figure. Near Verbania (8.55°E), intense updrafts (closely flanked by downward motion) are apparent at 18:30 UTC (thus, slightly later compared to the observations). Hence, the model seems able to reproduce the vigorous convective activity in the study area nearly at the right time. In the following subsection, we will analyse the conditions responsible for such an intense vertical motion.

6.3. Instability parameters

Hereafter, the analysis of some instability parameters will allow to better understand the environmental conditions conducive to severe convection in this case. Fig. 16 shows the CAPE of the most unstable parcel (MUCAPE), as evaluated in the model outer grid at 18:00 UTC. An area of very high CAPE (> 3000 J/kg) affects the western Mediterranean, with a peak in the Tyrrhenian and in the Ligurian Seas; from this region, a tongue of warm and moist air propagates northward across the Ligurian coasts toward the Piedmont inland, enhancing the potential instability in the area.

Fig. 17 shows the 0–6 km wind difference (a), the 0–1 km Storm Relative Helicity (SRH), (b) the Energy Helicity Index (EHI) (c), and the K-index (d). All Figures refer to the inner grid (zoomed in the area of interest) at 18:30 UTC, 25 August, i.e. the time when the model simulates the maximum convective activity in the area (similar patterns are present in the pre-convective environment 30 min earlier, suggesting that the high values are not affected yet by the developing convection).

In severe convective events, strong vertical wind shear enables longer storm lifetime and supports organized convective systems (e.g., supercells) that influence the severity of the storm (Markowski and Richardson, 2010). One can see, in Fig. 17a, that the simulated 0–6 km wind difference in the area near Verbania was favourable to the supercell development, since it was greater than 30 m/s (a value of 15–20 m/s is generally used as discriminant; Gordon and Albert, 2000; Miller, 1972; Rasmussen and Blanchard, 1998). Similarly, the vertical wind shear was high at low levels (not shown): the simulated wind difference between 0 and 1 km exceeds 12 m/s (values greater than 5–10 m/s are considered favourable for the development of supercell and tornadoes; Craven and Brooks, 2004), and is about 22 m/s in the layer 0–3 km. This is consistent with the remark that localized severe convection episodes in Italy, tornadoes in particular, are often associated with high values of low-level wind shear (Giaiotti et al., 2007; Miglietta and Rotunno, 2016).

As a consequence of the intense shear, the 1-km SRH, a measure of the potential for updraft rotation in supercells, reaches values up to 180 $m^2\ s^{-2}$ near Verbania (Fig. 17b), i.e. above the value of 100 $m^2\ s^{-2}$ generally associated with a high threat of tornado occurrence

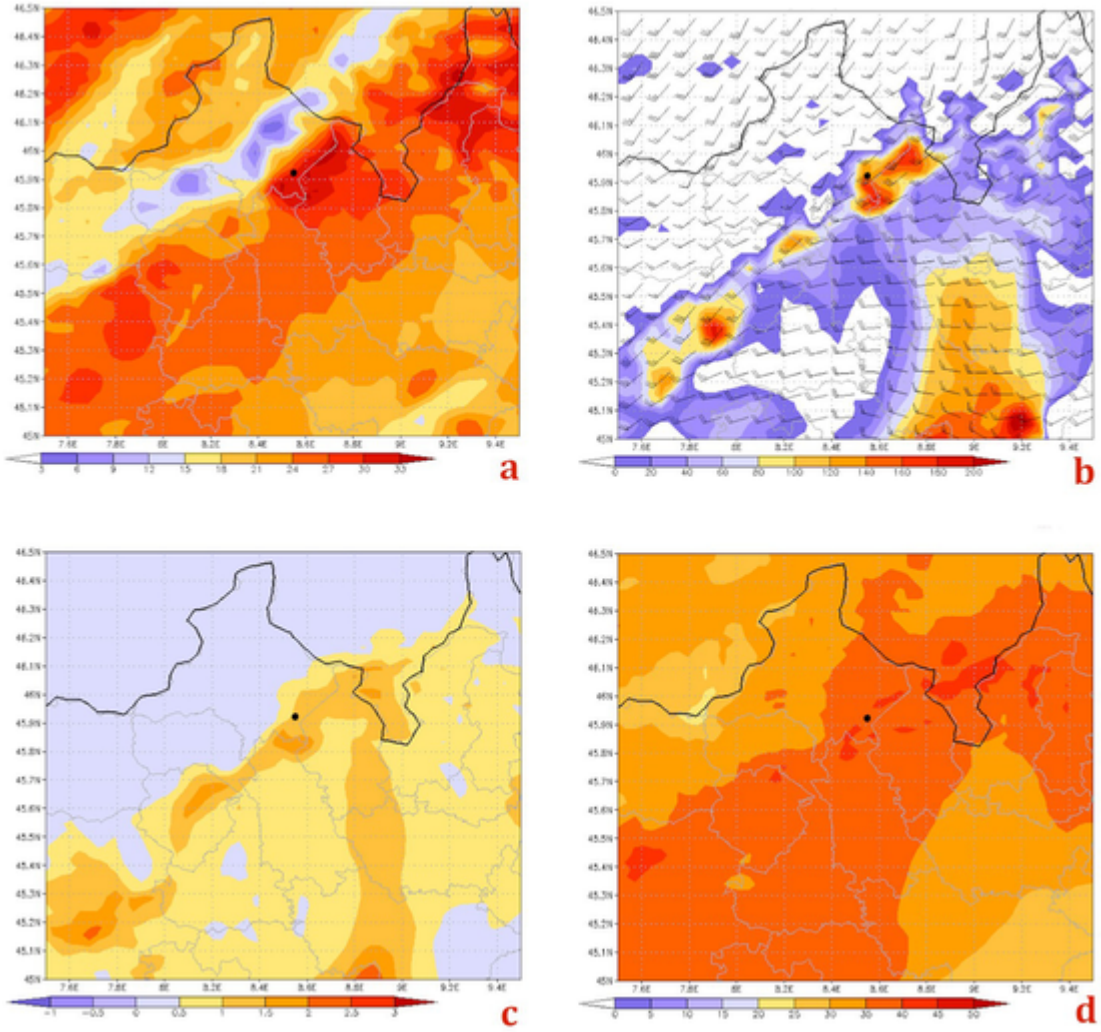

Fig. 17. WRF-inner grid (zoom): (a) 0–6 km wind difference (m/s); (b) 1 km SRH (m^2/s^2); (c) EHI and (d) K-index (°C). All maps refer to 18:30 UTC, 25 August. The black dot denotes the position of Verbania. (For interpretation of the references to colour in this figure legend, the reader is referred to the web version of this article).

(Davies-Jones et al., 1990). Similarly, the Energy Helicity Index EHI = (CAPE*SRH)/($1.6*10^5$), i.e. a combination of instability and wind shear, is shown in Fig. 17c in the layer 0–3 km. The simulated EHI reaches a value of 2 in the area surrounding Verbania; again, this value is favourable to the development of cyclonic supercells (Davies, 1993).

Another useful diagnostic parameter related to the thunderstorm/convective potential is the K-index, based on the vertical temperature lapse rate, the moisture content of the lower troposphere, and the vertical extent of the moist layer. K is defined as: $K = (T_{850}-T_{500}) + Td_{850}-(T_{700}-Td_{700})$, where T is the temperature, Td the dew point and the subscript numbers represent the isobaric levels (hPa). Fig. 17d shows that the simulated value was locally above 45 °C, which denotes a high potential for convective development and thunderstorms with heavy rain (George, 1960).

Very high values are also simulated for other instability parameters (not shown), such as the Total Totals (locally greater than 55 °C) and the Integrated Water Vapour (IWV; around 50 mm). In particular, the latter value is really extreme, suggesting that a huge amount of humidity was available in the vertical column to feed convection.

We summarize in Table 1 the values of the instability indices calculated in the surrounding of the Lake Maggiore, as derived from the WRF model output. The interpretation provided in Table 1 refers to the comparison with the climatology derived from studies mainly focused on the USA, whereas the thresholds for severe weather are generally higher than in Europe (cf. Brooks, 2009 with Romero et al., 2007). Nevertheless, the instability indices for the present case study appear relevant even in comparison with the USA climatology.

Table 1
Summary of the main instability indices simulated by WRF in the Lake Maggiore area at 18:30 UTC, 25 August 2012.

Instability Indices	WRF (simulated values in the surroundings of Verbania at 18:30 UTC, 25 August 2012)	Interpretation
MUCAPE	700–1000 J/kg	*moderate instability*
CIN	40 J/kg	*moderate-to-strong inhibition*
0–6 km Shear	30–33 m/s	*supercell potential*
0–3 km Shear	20–22 m/s	*supercell potential*
0–1 km Shear	12–13 m/s	*supercell potential*
0–3 km SRH	> 300 m^2/s^2	*possible mesocyclone formation. Significant tornadic supercells likely*
0–1 km SRH	180 m^2/s^2	*possible mesocyclone formation. Significant tornadic supercells likely*
IWV	50 mm	*huge amount of humidity available in the vertical column (High Precipitation supercell)*
K-index	40–45 °C	*high convective potential*
Sweat	350–400	*severe thunderstorms / tornado possible*
T-Totals	> 55 °C	*severe thunderstorms likely*
EHI	1–2	*mesocyclone-induced tornadoes possible*

6.4. Supercell identification

The Updraft helicity (UH) is a diagnostic field introduced in Kain et al. (2008) in order to track rotation in simulated storms; it is calculated taking the integral of the vertical vorticity times the updraft velocity between 2 and 5 km AGL. Several studies have demonstrated the utility of UH in predicting tornado severity (Clark et al., 2012). In our case, this parameter is examined to identify a possible mesocyclonic circulation indicative of the presence of a supercell, as that present in the Doppler radar velocity, and to track its motion over the area of Verbania.

Fig. 18 shows the UH simulated by WRF at 18:30 (Fig. 18a) and 19:00 (Fig. 18b) UTC: the sequence shows the northeastward motion of the cell crossing Verbania, with an estimated translation speed of more than 10 m/s and values of UH greater than 100 m^2/s^2, denoting intense helicoidal ascending motion typical of a well-developed supercell. Fig. 19a (18:30 UTC) and 19b (19:00 UTC) show the storm-relative velocity, obtained by subtracting the translational motion of the cell from the horizontal wind, together with the 700 hPa vertical wind component. These Figures show the presence of rotation in the cell, occurring during its translation from SW to NE, together with the presence of an updraft and a downdraft near the centre. The presence of a main updraft on the southeastern side of the storm and of large areas of downdrafts on the west and north side, are typical of mesocyclones (Klemp, 1987). The region of descending currents, consisting of dry air wrapping around the cell, is often

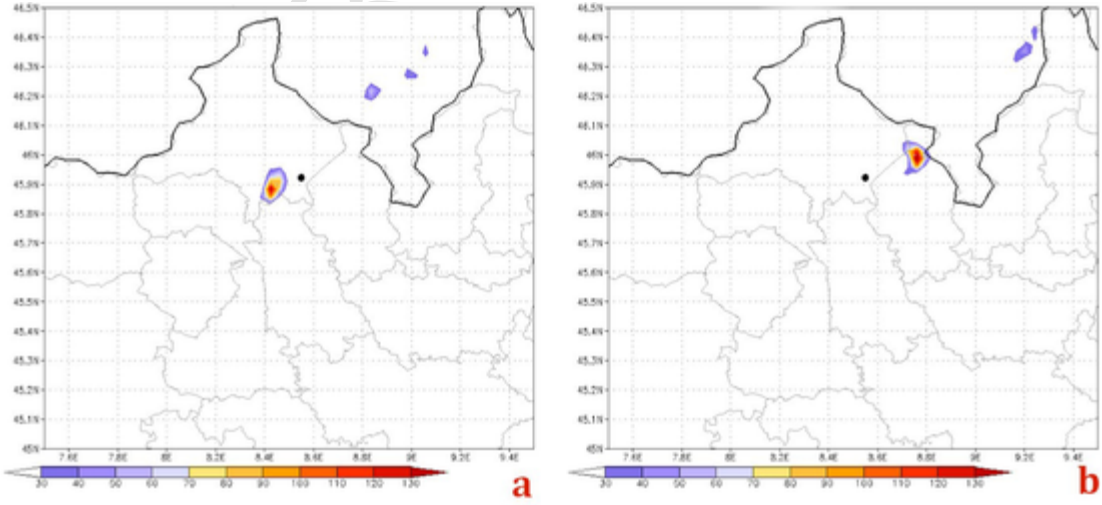

Fig. 18. WRF-inner grid (zoom) updraft helicity (shaded; values >30 m^2/s^2) at 18:30 UTC (a) and 19:00 UTC (b), 25 August. The black dot denotes the position of Verbania. (For interpretation of the references to colour in this figure legend, the reader is referred to the web version of this article).

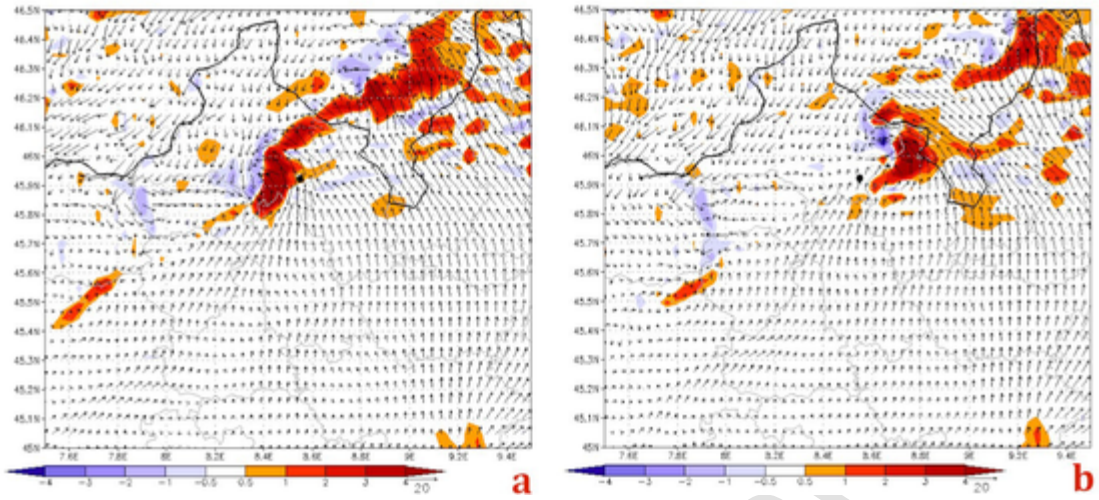

Fig. 19. WRF-inner grid (zoom) 700 hPa vertical wind speed (colours, m/s) and "storm-relative" wind (vectors), at 18:30 UTC (a) and 19:00 UTC (b), 25 August. The black dot denotes the position of Verbania. (For interpretation of the references to colour in this figure legend, the reader is referred to the web version of this article).

characterized by heavy rain and hail, and has been correlated to tornado formation when concomitant with radar hook echoes (Fujita, 1975; Lemon and Doswell, 1979; Davies-Jones, 1982).

7. Conclusions

A detailed analysis of the meteorological conditions that led to a severe storm in northwestern Italy (Lake Maggiore area) on 25 August 2012, characterized by heavy rain, hail and strong wind gusts, is presented. The study was carried out through an integrated approach that involves numerical simulations, satellite and radar data, and surface/upper air measurements.

The synoptic analysis reveals that the intrusion of cooler air at mid-upper levels, the presence of a jet stream over the Lake Maggiore area, along with very hot and humid air in the PBL, helped to create conditions of high potential instability. The mechanical forcing of the nearby orography triggered convection, while the warm surface of Lake Maggiore possibly contributed to remove the thermal inversion and created a low-level environment favourable to the development of severe convection.

High-resolution WRF model numerical simulations showed that the environment of the event was successfully reproduced. High values of several instability parameters, usually adopted in convective analysis, were simulated; the values were above the typical thresholds considered for the occurrence of severe weather.

The satellite analysis confirmed that severe convective processes were active, characterized by intense updrafts that penetrated into the lower stratosphere. After a rapid cloud top cooling, the storm assumed a cold-U shaped signature, which later developed into a cold-ring shape; both features are typical of severe convection and indicate the presence of an intense updraft.

Reflectivity and Doppler radar velocity data allowed to identify the development of an intense storm characterized by internal rotation, suggesting the presence of a mesocyclone. A specific Thunderstorm Radar Tracking algorithm reconstructed the storm motion, confirming the results emerging from the updraft helicity and storm-relative velocity simulated with the WRF model. An increase in hail activity was shown when the storm moved near Verbania, suggesting that the updraft was well organized and strong enough to sustain a hail core. The radar-based hail size estimation (MESHS) showed that hail stones were initially small (< 2 cm), while greater hail sizes (till 5–6 cm) were produced 20–30 min after the storm passed over Verbania. This is an indication that the storm had a strong and persistent updraft for some tens of minutes.

Although radar data and WRF model simulations agree in identifying a mesocyclonic circulation, and the first damage survey suggested the possible coexistence of a tornado and a downburst, we cannot draw definitive conclusions about the exact nature of the event. Possibly, very high-resolution numerical simulations (grid spacing of the order of 100 m) would be required to better understand the nature of the event and to determine its character, i.e. linear (downburst) or rotational (tornado).

Declaration of Competing Interest

The authors declare that they have no known competing financial interests or personal relationships that could have appeared to influence the work reported in this paper.

Acknowledgments

LINET data were provided by Nowcast GmbH (https://www.nowcast.de/) within a scientific agreement between H.-D. Betz and the Satellite Meteorological Group of CNR-ISAC in Rome. The Regional Agency for the Protection of the Environment of Piedmont region (ARPA Piemonte) is acknowledged for the radar images and for surface data. Special thanks to IRSA-CNR, former ISE-CNR, for the surface data on Verbania Pallanza, and to the Italian Department of Civil Protection for the observed precipitation map (derived by the automatic system Dewetra).

References

ARPA Piemonte (The Regional Agency for the Protection of the Environment of Piedmont) Event Analysis available on linehttp://www.arpa.piemonte.it/approfondimenti/temi-ambientali/meteorologia-e-clima/meteo/documenti-e-dati/evento_25_08_2012.pdf2012last access 31 Dec 2019

Avolio, E, Federico, S, 2018. WRF simulations for a heavy rainfall event in southern Italy: Verification and sensitivity tests. Atmos. Res. 209, 14–35.

Avolio, E, Federico, S, Miglietta, M M, Lo Feudo, T, Calidonna, C R, Sempreviva, A M, 2017. Sensitivity analysis of WRF model PBL schemes in simulating boundary-layer variables in southern Italy: an experimental campaign. Atmos. Res. 192, 58–71.

Betts, A K, Miller, M J, 1986. A new convective adjustment scheme. Part II: Single column tests using GATE wave, BOMEX, ATEX and arctic air-mass data sets. Q. J. R. Meteorol. Soc. 112, 693–709.

Betz, H-D, Schmidt, K, Laroche, P, Blanchet, P, Oettinger, P, Defer, E, Dziewit, Z, Konarski, J, 2009. LINET-an international lightning detection network in Europe. Atmos. Res. 91, 564–573.

Brooks, H E, 2009. Proximity soundings for severe convection for Europe and the United States from reanalysis data. Atmos. Res. 93, 546–553.

Brunner, J C, Ackerman, S A, Bachmeier, A S, Rabin, R M, 2007. A quantitative analysis of the enhanced-V Feature in relation to severe weather. Wea. Forecast. 22, 853–872.
Clark, A J, Kain, J S, Marsh, P T, Correia, J, Jr., Xue, M, Kong, F, 2012. Forecasting tornado pathlengths using a three-dimensional object identification algorithm applied to convection-allowing forecasts. Wea. Forecast. 27, 1090–1113.
Craven, J P, Brooks, H E, 2004. Baseline climatology of sounding derived parameters associated with deep moist convection. Natl. Weather Dig. 28, 13–24.
Davies, J M, 1993. Small tornadic supercells in the central plains. Preprints. In: 17th Conf. Severe Local Storms, St. Louis, MO, Amer. Meteor. Soc, pp. 305–309.
Davies-Jones, R P, 1982. Observational and theoretical aspects of tornadogenesis. In: Bengtsson, L, Lighthill, J (Eds.), Intense Atmospheric Vortices. Springer-Verlag, pp. 175–189.
Davies-Jones, R, Burgess, D W, Foster, M, 1990. Test of helicity as a forecast parameter. In: Preprints, 16th Conf. on Severe Local Storms, Kananaskis Park, AB, Canada, Amer. Meteor. Soc. pp. 588–592.
Doswell, C A, III, Carbin, G W, Brooks, H E, 2012. The tornadoes of spring 2011 in the USA: an historical perspective. Weather 67, 88–94.
Dotzek, N, Groenemeijer, P, Feuerstein, B, Holzer, A M, 2009. Overview of ESSL's severe convective storms research using the European Severe Weather Database ESWD. Atmos. Res. 93, 575–586.
Fujita, T T, 1975. New evidence from the April 3–4, 1974 tornadoes. In: Preprints, Ninth Conf. on Severe Local Storms, Norman, OK, Amer. Meteor. Soc. pp. 248–255.
George, J J, 1960. Weather Forecasting for Aeronautics. Academic press, p. 673.
Germann, U, Boscacci, M, Gabella, M, Sartori, M, 2015. Radar design for prediction in the Swiss Alps. Meteor. Technol. Int. 4, 42–45.
Giaiotti, D B, Giovannoni, M, Pucillo, A, Stel, F, 2007. The climatology of tornadoes and waterspouts in Italy. Atmos. Res. 83, 534–541.
Gianfreda, F, Miglietta, M M, Sansò, P, 2005. Tornadoes in southern Apulia (Italy). Nat. Hazards 34, 71–89.
Gordon, J, Albert, D, 2000. A Comprehensive Severe Weather Fore-Cast Checklist and Reference Guide. Noaa technical service publication TSp 10, NWS central region.
Hering, A M, Germann, U, Boscacci, M, Sénési, S, 2008. Operational nowcasting of thunderstorms in the Alps during MAP D-PHASE. In: Proceedings of 5th European Conference on Radar in Meteorology and Hydrology (ERAD), 30 June–4 July 2008, Helsinki, Finland. Copernicus: Göttingen. pp. 1–5.
Homar, V, Gayà, M, Romero, R, Ramis, C, Alonso, S, 2003. Tornadoes over complex terrain: an analysis of the 28th August 1999 tornadic event in eastern Spain. Atmos. Res. 67–68, 301–317.
Iacono, M J, Delamere, J S, Mlawer, E J, Shephard, M W, Clough, S A, Collins, W D, 2008. Radiative forcing by long–lived greenhouse gases: calculations with the AER radiative transfer models. J. Geophys. Res. 113, D13103.
Isotta, F A, Frei, C, Weilguni, V, Tadić, M P, Lassegues, P, Rudolf, B, Pavan, V, Cacciamani, C, Antolini, G, Ratto, S M, Munari, M, Micheletti, S, Bonati, V, Lussana, C, Ronchi, C, Panettieri, E, Marigo, G, Vertačnik, G, 2014. The climate of daily precipitation in the Alps: development and analysis of a high-resolution grid dataset from pan-Alpine rain-gauge data. Int. J. Climatol. 34, 1657–1675.
James, N C, Houze, R A, 2001. A real-time four-dimensional doppler dealiasing scheme. J. Atmos. Ocean. Technol. 18, 1674–1683.
Jansà, A, Alpert, P, Arbogast, P, Buzzi, A, Ivancan-Picek, B, Kotroni, V, Llasat, M, Ramis, C, Richard, E, Romero, R, et al., 2014. MEDEX: a general overview. Nat. Hazards Earth Syst. Sci. 14 (8), 1965–1984.
Jirak, I L, Cotton, W R, McAnelly, R L, 2003. Satellite and radar survey of mesoscale convective system development. Mon. Weather Rev. 131, 2428–2449.
Kain, J S, et al., 2008. Some practical considerations regarding horizontal resolution in the first generation of operational convection-allowing NWP. Wea. Forecast. 23, 931–952.
Klemp, J B, 1987. Dynamics of tornadic thunderstorms. Annu. Rev. Fluid Mech. 19, 369–402.
Lemon, Doswell, C A, 1979. Severe thunderstorm evolution and mesocyclone structure as related to tornadogenesis. Mon. Weather Rev. 107, 1184–1197.
Lionello, P, et al., 2006. The Mediterranean climate: An overview of the main characteristics and issues. In: Mediterranean Climate Variability, Eds. Elsevier, pp. 1–26.
Markowski, P, Richardson, Y, 2010. Mesoscale meteorology in midlatitudes. John Wiley & Sons, p. 420.
Matsangouras, I T, Nastos, P T, Bluestein, H B, Sioutas, M V, 2014. A climatology of tornadic activity over Greece based on historical records. Int. J. Climatol. 34, 2538–2555.
Matsangouras, I T, Nastos, P T, Bluestein, H B, Papachristopoulou, K, Pytharoulis, I, Miglietta, M M, 2017. Analysis of waterspout environ- mental conditions and of parent-storm behaviour based on satellite data over the southern Aegean Sea of Greece. Int. J. Climatol. 37, 1022–1039.
McDonald, J, Mehta, K C, 2006. A recommendation for an Enhanced Fujita Scale (EF-Scale). Revision 2 Wind Science and Engineering Research Center, Texas Tech University, p. 111.
Miglietta, M M, Matsangouras, I T, 2018. An updated "climatology" of tornadoes and waterspouts in Italy. Int. J. Climatol. 1–17.
Miglietta, M M, Rotunno, R, 2016. An EF3 multivortex tornado over the Ionian region: is it time for a dedicated warning system over Italy? Bull. Am. Meteorol. Soc. 97, 337–344.
Miglietta, M M, Manzato, A, Rotunno, R, 2016. Characteristics and predictability of a supercell during HyMeX SOP1. Q. J. Roy. Meteor. Soc. 142, 2839–2853.
Miglietta, M M, Mazon, J, Rotunno, R, 2017. Numerical Simulations of a Tornadic Supercell over the Mediterranean. Wea. Forecast. 32, 1209–1226.
Miglietta, M M, Mazon, J, Motola, V, Pasini, A, 2017. Effect of a positive Sea Surface Temperature anomaly on a Mediterranean tornadic supercell. Sci. Rep. 7 (12828), 1–8.
Miller, R C, 1972. Notes on analysis and severe storm forecasting procedures of the Air Force Global Weather Center, AWS Tech. Report 200 (Rev.), Headquarters Air Weather Service, Scott AFB. p. 106.
Nisi, L, Martius, O, Hering, A, Kunz, M, Germann, U, 2016. Spatial and temporal distribution of hailstorms in the Alpine region: a long-term, high resolution, radar-based analysis. Q. J. R. Meteorol. Soc. 142 (697), 1590–1604.
Nisi, L, Hering, A, Germann, U, Martius, O, 2018. A 15-year hail streak climatology for the Alpine region. Q. J. R. Meteorol. Soc. 144 (714), 1429–1449.
Panziera, L, Germann, U, 2010. The relation between airflow and orographic precipitation on the southern side of the Alps as revealed by weather radar. Q. J. R. Meteorol. Soc. 136 (646), 222–238.
Panziera, L, Gabella, M, Germann, U, Martius, O, 2018. A 12-year radar-based climatology of daily and sub-daily extreme precipitation over the Swiss Alps. Int. J. Climatol. 38 (10), 3749–3769.
Panziera, L, James, C N, Germann, U, 2015. Mesoscale organization and structure of orographic precipitation producing flash floods in the Lago Maggiore region. Q. J. R. Meteorol. Soc. 141 (686), 224–248.
Peyraud, L, 2013. Analysis of the 18 July 2005 Tornadic Supercell over the Lake Geneva Region. Wea. Forecast. 28, 1524–1551.
Pleim, J E, 2007. A combined local and non-local closure model for the atmospheric boundary layer. Part 1: model description and testing. J. Appl. Meteorol. Climatol. 46, 1383–1395.
Rasmussen, E N, Blanchard, D O, 1998. A baseline climatology of sounding-derived supercell and tornado forecast parameters. Wea. Forecast. 13, 1148–1164.
Rodríguez, O, Bech, J, 2018. Sounding-derived parameters associated with tornadic storms in Catalonia. Int. J. Climatol. 38, 2400–2414.
Romero, R, Gaya, M, Doswell, C A, III, 2007. European climatology of severe convective storm environmental parameters: a test for significant tornado events. Atmos. Res. 83, 389–404.
Scheffkneckt, P, Serafin, S, Grubisic, V, 2017. A long-lived supercell over mountainous terrain. Q. J. R. Meteorol. Soc. 143, 2973–2986.
Schenkman, A D, Xue, M, Shapiro, A, Brewster, K, Gao, J, 2011. The analysis and prediction of the 8-9 may 2007 Oklahoma tornadic mesoscale convective system by assimilating WSR-88D and CASA radar data using 3DVAR. Mon. Weather Rev. 139 (1), 224–246.
Setvák, M, Lindsey, D T, Novák, P, Wang, P K, Radová, M, Kerkmann, J, Grasso, L, Su, S-H, Rabin, R M, Šťástka, J, Charvát, Z, Kyznarová, H, 2010. Satellite-observed cold-ring-shaped features atop deep convective clouds. Atmos. Res. 97, 80–96.
Skamarock, W C, Klemp, J B, Dudhia, J, Gil, D A, Barker, D M, Duda, M G, Huang, X Y, Wang, W, Powers, J G, 2008. Description of the Advanced Research WRF Version 3. National Center for Atmospheric Research. Boulder, Colorado, USA.
Tewari, M, Chen, F, Wang, W, Dudhia, J, LeMone, M A, Mitchell, K, Ek, M, Gayno, G, Wegiel, J, Cuenca, R H, 2004. Implementation and Verification of the Unified NOAH Land Surface Model in the WRF Model. In: 20th Conference on Weather Analysis and Forecasting/16th Conference on Numerical Weather Prediction. Pp. pp. 11–15.
Thompson, G, Field, P R, Rasmussen, R M, Hall, W D, 2008. Explicit forecasts of winter precipitation using an improved bulk microphysics scheme. Part II: implementation of a new snow parameterization. Mon. Weather Rev. 136, 5095–5115.
Wallace, J M, Hobbs, P V, 2006. Atmospheric Science: An Introductory Survey. Elsevier Academic Press, Amsterdam.
Zanini, M A, Hofer, L, Faleschini, F, Pellegrino, C, 2017. Building damage assessment after the Riviera del Brenta tornado, Northeast Italy. Nat. Hazards 86, 1247–1273.